Early age movement in offshore structures with various bearing conditions

Early age movement in offshore structures with various bearing conditions

Henneberg, Joshua; Schaumann, Peter

Institute for Steel Construction – Forwind
Appelstraße 9A
30167 Hannover
Germany

henneberg@stahl.uni-hannover.de

Abstract. Grouted connections (GCs) consist of two infiltrating steel tubes of different diameters and a grout material bonding the two steel tubes together. Predominantly, the GCs are used to connect the foundation piles with the jacket support structure. Additionally, it can be applied for monopile substructures. A challenging and scientifically still marginally analysed detail of grouted connections is the influence of early age movement (EAM), also known as early age cycling (EAC) on the final load bearing behaviour of the connection. After grouting and until the end of the curing of the material, the offshore structure is partially supported by fluid grout material for several hours. During this time waves and current affect the soft connections. This leads to relative movement during the curing of GCs, which is known as EAM. Previous investigations showed grout material damage due to vertical EAM. These results form the basis of the current offshore guideline limits. According to DNVGL-OS-J101 from 2014, it must be ensured that during the curing process the vertical EAM does not exceed 1 mm. Since 2016 the limit value also applies for the lateral EAM according to DNVGL. However, the influence of lateral EAM on the load bearing behaviour is barely experimentally nor numerically investigated. Thus, the authors are involved in a comprehensive research project (GREAM) addressing this topic. This paper focusses on Finite Element Analysis of different support structures under varying boundary conditions and sea states to analyse the amplitude of lateral EAM of grouted connections.

1. Introduction

GCs are hybrid connections which have been used offshore in bottom-fixed structures for years [1]. It is a robust pile-sleeve connection in which two steel tubes of different diameters (smaller = pile; larger = sleeve) are connected via a grout layer. In order to increase the resistance, shear keys are placed on the facing surfaces. Depending on the substructure, the GCs can be conical and designed without shear keys as well. These hybrid connections have several advantages in rough offshore conditions.

Typical offshore structures with GCs are monopiles and pre- or post-piled jackets for offshore wind turbines (OWT) and converter platforms / substations (OSS); cf. figure 1. For jacket structures the GC is the predominantly used connection type due to the complex installation procedure at mudline level and the difficult inspection conditions. Designers lost confidence in the GC designs for monopile support structures ten years ago, when a huge number of cylindrical GCs without shear keys slipped [6]. This is the reason that new offshore farms with monopiles are realized predominantly with a ring flange connection even if a development to cylindrical GC with shear keys in the middle third of the grout

length and conical GC without shear keys would be possible; cf. Figure 4. Only a few monopile structures are realized with GCs.

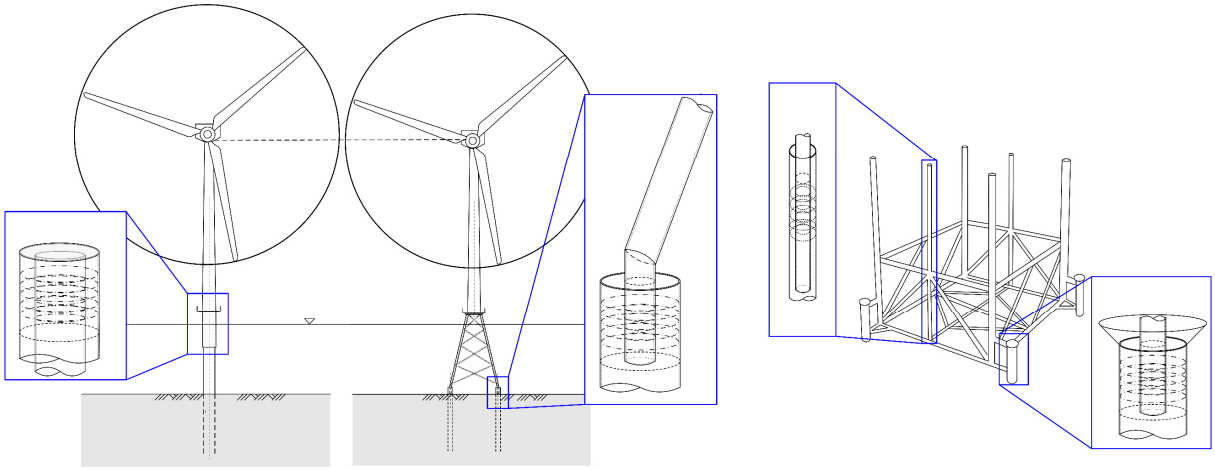

Figure 1. Offshore support structures with grouted connections (left: monopile, middle: jacket for OWT and right: jacket for OSS).

For increasingly larger and optimized offshore structures, problems with early age movement / cycling (EAM / EAC) during the curing of GCs are becoming more evident. Based on experimental investigations by Wimpey in 1986 [2] and DNV in 1994 [3], limit values for EAM were included into various offshore guidelines (DNVGL [4-5] and EN ISO 19902 [7]). In the corresponding tests, the GCs were disturbed by vertical cyclic relative displacement in the range of ±1mm over the first 24 hours after grouting and then tested for their ultimate limit state after 28 days. On this basis, the guidelines evolved towards a limit value of 1mm relative displacement between the steel components of the GCs occurring in the first 24 h after grouting. These movements can be vertical or horizontal and have to be proven by on-bottom analyses of the offshore structure with ungrouted piles [5]. If the limit value is exceeded, appropriate mechanical countermeasures have to be taken, the installation window (usually sea states of 2.5 to 3m significant wave height) has to be restricted or the corresponding sections of the grouted connection have to be considered as not supporting [5] or reduced by a factor according to [7]. Confinements in the weather window can be associated with high costs, since it can lead to significant delays in the project schedule and consequently high rents for the installation vessels.

2. Wave loading

EAM is predominately caused by the sea state, since tower and turbine are not jet installed. Changing wind loads are neglected due to the small attacking area. To reduce installation inaccuracies, sea states of up to 3m significant wave height are investigated; cf. table 1. According to FINO 1 data [8], the following sea states are investigated to evaluate the risk of EAMs greater than the limit of 1mm according DNVGL [5].

Table 1. Waves according to FINO 1 met mast data (German North Sea) [8]

Significant wave height [m]	0.5	1.0	1.5	2.0	2.5	3.0
Peak period [s]	6.21	6.24	6.67	7.30	7.86	8.47

As the following sea state simulations differ in local, global as well as elastic deformation and rigid body movement, the methods of applying the wave loading differs between simulations. On the one hand, the potential theory (Equation 1 and 2) is used to apply the local pressure distribution on the shaft of the steel tubes according to [9]; cf. section 3.

$$p = -\rho \frac{\partial \phi}{\partial t} \tag{1}$$

$$\phi = -i\frac{gH}{2\omega} \cdot \frac{cosh(k(z+h))}{cosh(kh)} \sum_{p=0}^{\infty} \epsilon_p i^p \left[J_p(kr) - \frac{J'_{(kr_0)}}{H_p^{(1)'}(kr_0)} H_p^{(1)}(kr) \right] cos(p\theta)\, e^{-i\omega t} \tag{2}$$

This theory is used to enable a realistic pressure distribution on slender offshore structures according to wave loading, which is predominately caused by the inertia term of the wave loading; cf. Figure 2. The blue triangle represents the range of the investigated monopile structures and the red rhombus represents the investigated jacket structures.

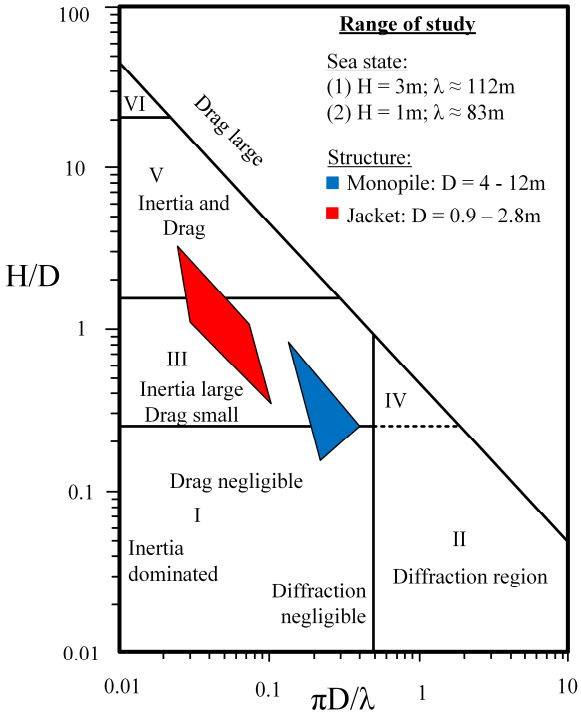

Figure 2. Rates of drag, inertia and diffraction for the wave loading on a cylinder according to Chakrabarti (Chakrabarti,1987) with coloured areas for different ranges of the current study.

On the other hand, the wave loading on tubular elements with small diameters, among which most jackets belong, is realised by the Morison Equation [10]. The wave loading is divided into the inertia force f_M and the drag force f_D; cf. Equation 3.

$$f(t) = f_M + f_D = c_M \cdot \rho \cdot \frac{\pi \cdot D^2}{4} \cdot \frac{\partial u(t)}{\partial t} + c_D \cdot \frac{\rho}{2} \cdot D \cdot |u(t)| \cdot u(t) \tag{3}$$

The wave force *f(t)* is calculated according to the time dependent water particle velocity *u(t)*, the coefficients (C_D and C_M) used according to DNVGL-ST-0126 c_M = 2.0 and c_D = 0.7 for smooth steel cylinders while installation and density of water ρ as well as the attacking surface equivalent with the diameter *D* of the steel tube. Sea states are considered through the JONSWAP spectrum [11], which is in accordance with the German North Sea. All simulations are performed with the simulation software ANSYS Workbench 2020 R2. Rigid body simulations and pressure distributions on a pile are realised by using ANSYS AQWA (diffraction and response analyses) and ACT LoadMapping + ANSYS Mechanical. The elastic simulations of the jacket support structures are done by using ANSYS Mechanical in combination with ACT Offshore; cf. figure 3.

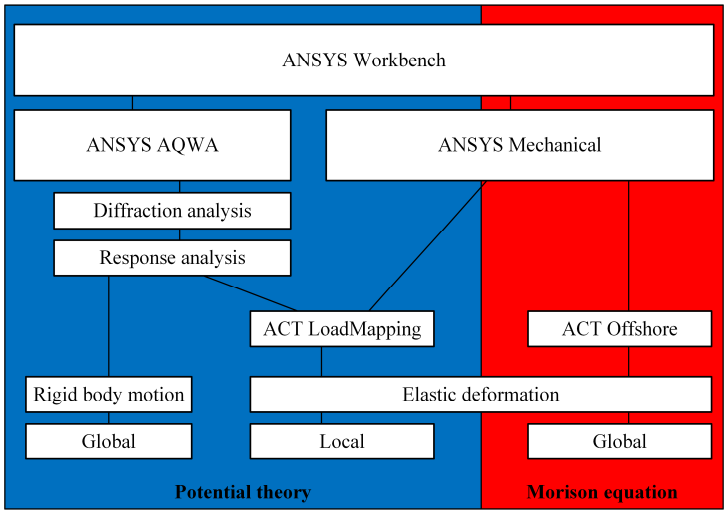

Figure 3. Workflow for different wave simulations with ANSYS Workbench 2020 R2 (blue: Potential theory and red: Morison equation).

3. Numerical investigation of EAM at monopile support structures

Typical GCs of monopile support structures are cylindrical steel tubes with shear keys in the middle third of the grout length or conical steel tubes without shear keys; cf. Figure 4. For positioning and leveling of the transition piece to adjust ramming inclinations, vertical brackets are used as temporary bearing for the transition piece until the grout material is hardened. Further horizontal brackets can be used for increasing safety issues during installation in earthquake-prone regions or to decrease EAM; cf. section 3.2. and 3.3.

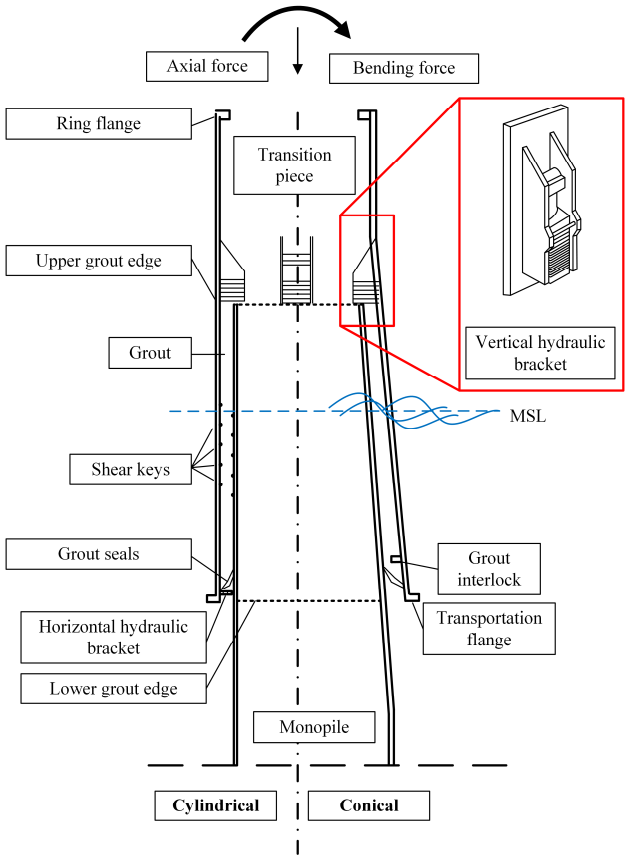

Figure 4. Typical grouted connections between transition piece and monopile.

3.1. Finite element model description

According to Lohaus et al. [8], the EAM at the transition piece of the monopile support structures is investigated, applying a more realistic wave loading approach, considering inertia loads by the potential theory, cf. Equation (1) and (2). During the installation process of the substructure, the transition piece is positioned on the top of the monopile by vertical brackets, which can differ in their amount (usually 3 to 6). figure 5 and table 2 show the numerical model used for the sensitivity analysis and the changing geometry parameters. The resistance of the fluid grout material is neglected.

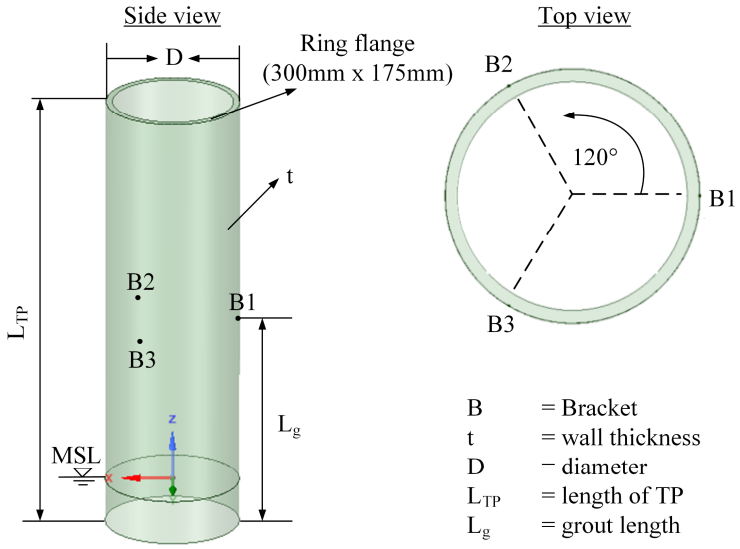

Figure 5. Model description investigations of monopile support structure

Table 2. Parameter of parameter study.

TP diameter D_{TP} [m]	4	6	8	10	12
TP thickness t_{TP} [m]	50	70	90	110	120
Number of brackets [-]	3	6	-	-	-
Grout length L_G [m]	7.5	12.5	17.5	-	-

Additional parameters like water depth, influence of shear keys and the wave attacking angle, have been investigated, as these possibly could affect predominantly the elastic deformation behaviour of the transition piece; cf. section 3.2. All the parameters have a negligible influence on EAM.

3.2. Elastic deformation of the transition piece

First of all, it should be noted that a horizontal and rotational rigid body movement of the entire transition piece is prevented at the brackets. Rigid body movement is investigated in section 3.3. At the brackets, the displacement in all three directions is set to zero. Rotations are permitted. It has to be noted that the pressure distribution on the shaft surface of the TP comes from inertia loading only and the monopile deformation is considered to be zero, which is not necessarily a conservative approach, as additional bending from the monopile is neglected.

For the highest occurring deformation caused by a sea state with 3m significant wave height and a wave period of 8.47s, the radial deformation of the TP shaft with and without horizontal brackets is shown in Figure 6.

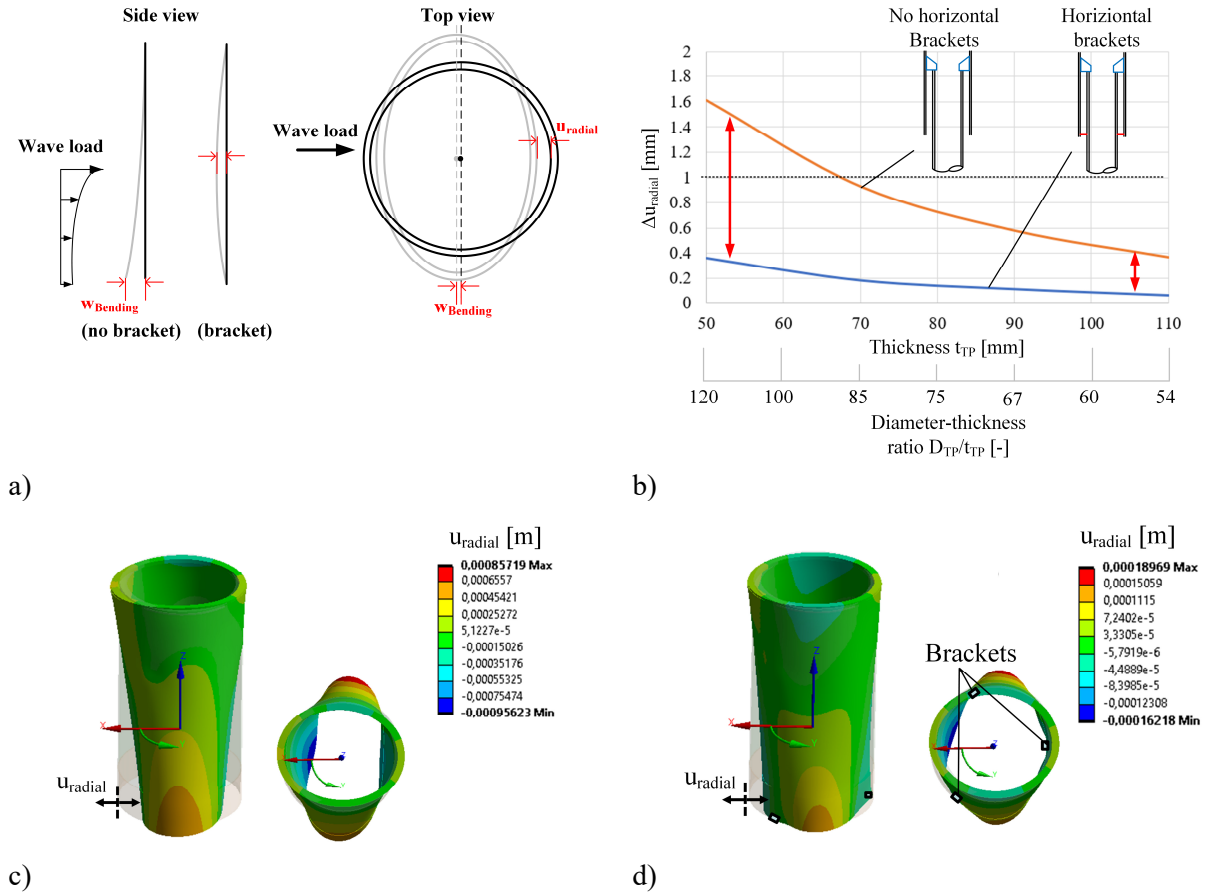

Figure 6. Possible EAM from elastic deformation (a), diagram showing the influence of thickness and horizontal brackets on EAM (b), Radial deformation of transition piece due to wave loading without (c) and with horizontal brackets (d).

As expected, the use of horizontal brackets reduces the EAM significantly, by about 75% for slender TPs and less pronounced for TPs with a lower slenderness. Analyses of different diameters D_{TP} leading to an EAM of 1.16mm, which is taken as reference value, show a dominating influence of D_{TP}. Increasing diameters lead to decreasing slenderness to fit the limits of EAM; cf. figure 7.

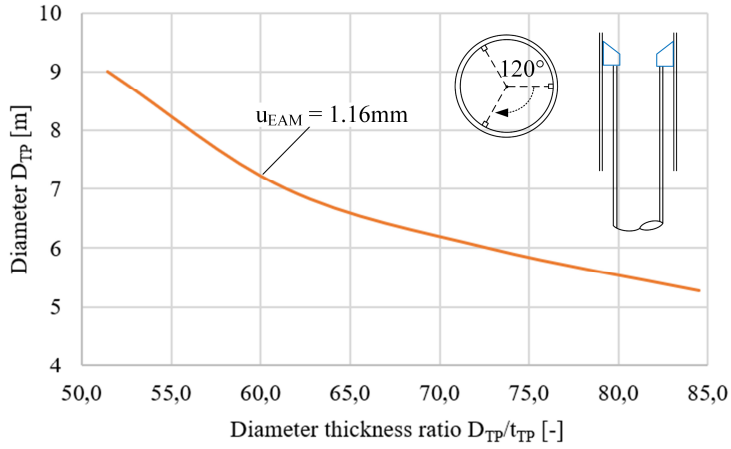

Figure 7. Influence of the diameter and thickness of the transition piece on the size of EAM

Further, increasing grout length L_G leads to an increasing EAM, as the distance between horizontal and vertical brackets increases. All in all, increasing sizes due to increasing OWT lead to increasing EAMs.

3.3. Rigid body movement of the transition piece

There are two different approaches to determine rigid body movement. One is a complex rigid body simulation to analyse if a rigid body movement occurs and how it develops over time, the other is a static equilibrium calculation to check whether movements occur or not. Before doing a complex rigid body simulation it is recommended to do the much simpler static equilibrium calculation as described in the following. There are two different possible rigid body movements to be checked. On the one hand side, there can be a translation, which occurs due to horizontal forces from the wave loading $F_{Destabil}$ according to Equation 3 are higher than the friction forces at the brackets $F_{Stabil} = F_{Weight} \cdot \mu$. On the other hand, a rotational rigid movement could occur, when the stabilizing moment M_{Stabil}, due to the dead load of the transition piece, taking possible eccentricity from secondary steel parts into account, are lower than the destabilizing moment coming from the wave loading $M_{Destabil}$.

$$\eta_{Toppling} = \frac{M_{Destablil}}{M_{Stabil}} \leq 1.0 \qquad or \qquad \eta_{Lateral} = \frac{F_{Destablil}}{F_{Stabil}} \leq 1.0 \tag{4}$$

Investigations from different transition pieces according to table 2, the risk of a rigid body movement is low for large TPs, whereas small/short TPs are prone to move as a whole. The utilization rate η ranges from 0.33 to 2.0; cf. figure 8 and 9. An increasing number of vertical brackets decrease the risk of toppling drastically; cf. figure 8.

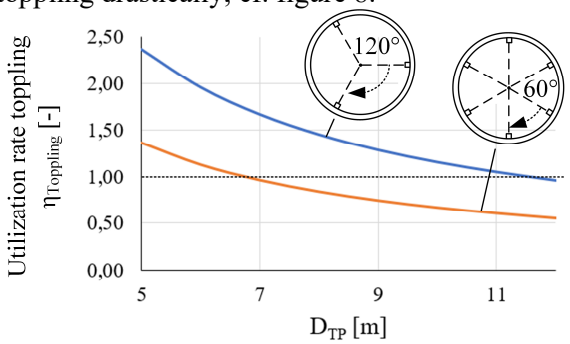

Figure 8. Influence of additional vertical brackets on toppling utilization.

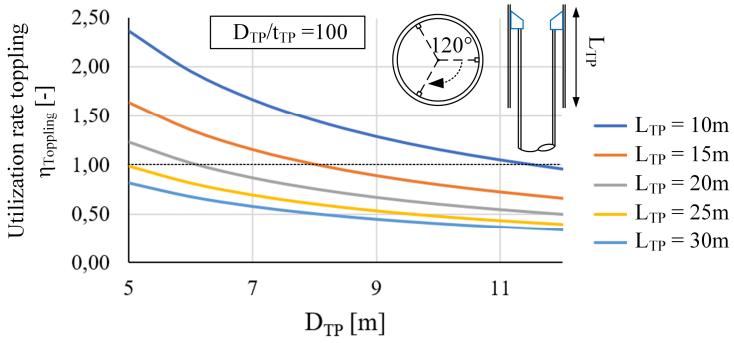

Figure 9. Influence of TP diameter on the risk of toppling

Rigid body simulations are possible, but as they need a lot of effort and a small increase of the wave loading leads to a significant increase of movement, the authors recommend designers to do static equilibrium calculations.

4. Numerical investigation of EAM at pre-piled jacket support structures

Comparable to the EAM at the transition piece of monopile support structures EAM occurs due to elastic deformation and rigid body motion at jacket support structures as well. In the following section elastic deformations of a pre-piled jacket (pin-in-pile connection) with a bearing according to the stopper and/or pile gripper is analyzed. Rigid body motion in lateral direction is disabled by the pile grippers, however would not occur due to the high dead load of the jacket and a comparably small horizontal loading from the waves ($\eta_{Lateral} \approx 0.1$).

4.1. Finite element model description

The analysed jacket has four legs and bays. It is placed in a water depth of 42m, has a total height of 60m and a foot print of 22m. The truss elements are implemented as tube elements with floodable chords and sealed braces. At the upper end of the grouted connection a hinged bearing is applied to consider the influence of stopper and pile gripper. On the save side no bending stiffness due to the pile gripper is considered.

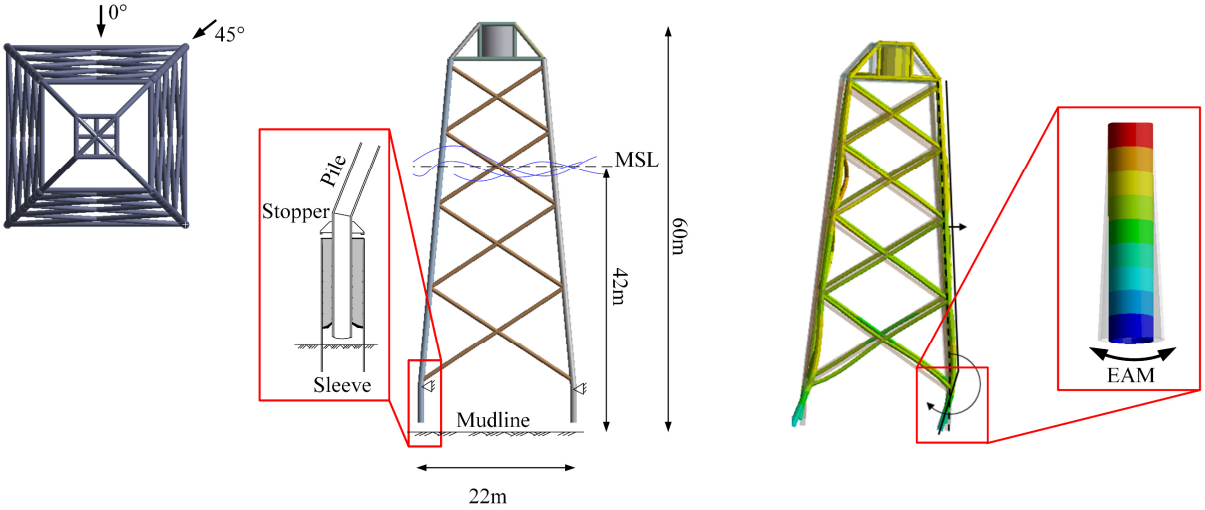

Figure 10. Linear elastic simulation of a pre-piled jacket structure (left: geometry and boundary conditions and right: elastic deformation leading to EAM).

The wave loading leads to a lateral deformation of the upper part of the jacket and local bending of the legs near the mudline. Inside the GC a pendular movement according to the cyclic characteristic of the wave loading occurs; cf. Figure 11.

Investigations on different wave angles (0° and 45°) showed 20% higher deformation due to wave loading from 45°. Some legs move in straight lines others follow an oval, due to structure wrapping; cf. figure 11. On the one hand, investigations on a stiffness increase due to additional horizontal bracings at the bottom DY-joint showed a significant decrease of the pendular movement in the GC by up to 40%. On the other hand, increasing the stiffness by the thickness t_{Leg} and the diameter D_{Leg} is shown in figure 12. The EAM is plotted over the resulting steel weight of the jacket chords and optional the lower horizontal braces to assess the different methods to decrease EAM economically. The smaller gradient of the dotted lines shows, that the stiffness increase by diameter is less efficient compared to a thickness increase, as increasing the diameter lead to an additional loading from the waves. Increasing the stiffness of the chords by thickness or an additional horizontal brace does lead to a small difference in point of view of material weight. As the horizontal braces increase welding time, lead to additional notches in a critical area as well as a small advantage in material savings to reach an equal Δu_{radial} and increasing the chord thickness leads to an additional increase of the fatigue resistance of the tubular steel joints [12] as well as a slightly smaller material fatigue behaviour, the authors think

both methods are suitable to prevent critical EAMs and have to be checked individually depending on the offshore project.

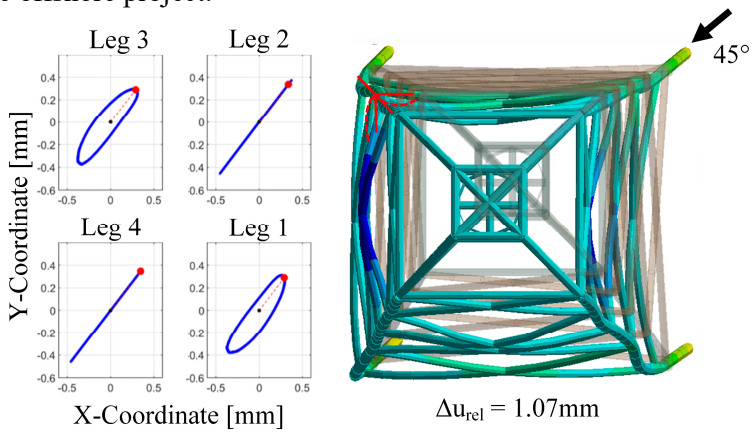

Figure 11. EAM at the bottom end of the jacket legs inside the GC under a wave coming from 45°.

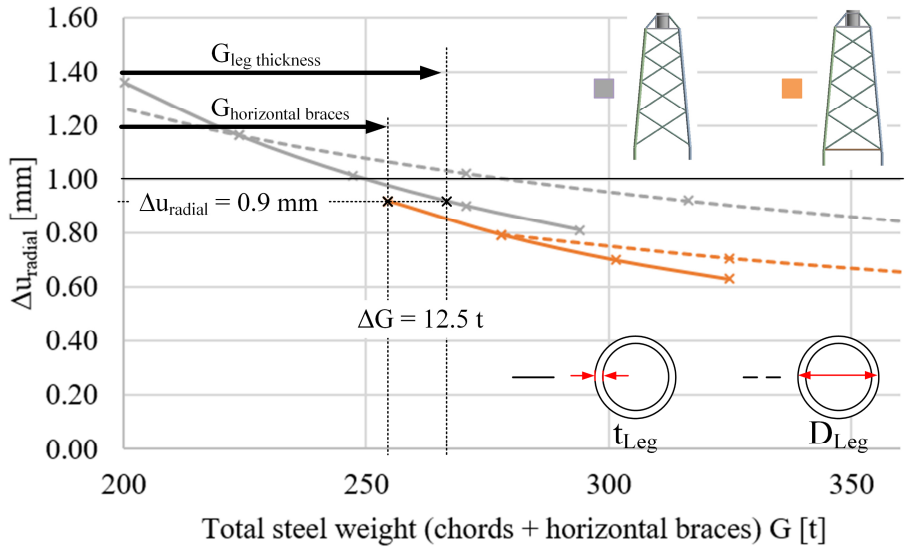

Figure 12. Changing jacket stiffness illustrated over total steel weight of legs and horizontal braces.

5. Numerical investigation of EAM at post-piled jacket support structures

Post-piled jackets are more prone to EAM according to a greater influence of structure-soil interaction, as the jacket is placed directly onto the seabed and in a second step the foundation piles are rammed. As the seabed has a low stiffness in the upper layers (few meters), small movements like EAM could occur. As a consequence, realistic boundaries for the on-bottom analysis have to be applied. Within this paper the pile-soil interaction is applied by the p-y method according to Sørensen [13] for cyclic loading, considering nonlinear spring behaviour in tension and compression direction. The spring data is calculated with the software IGtH-Pile 3.01 for uniform dense sand according to [14] over the total height. Additional bearings are applied as hinged connections between pile and jacket structure at the upper end of the skirt piles (pile gripper) and the upper end of the main piles (wedged). The simulations according to the sea state according to section 2, led to an EAM of 2mm at the lower end of the most loaded skirt pile and of 5.5mm at the middle part of the GC at the main piles; cf. figure 13.

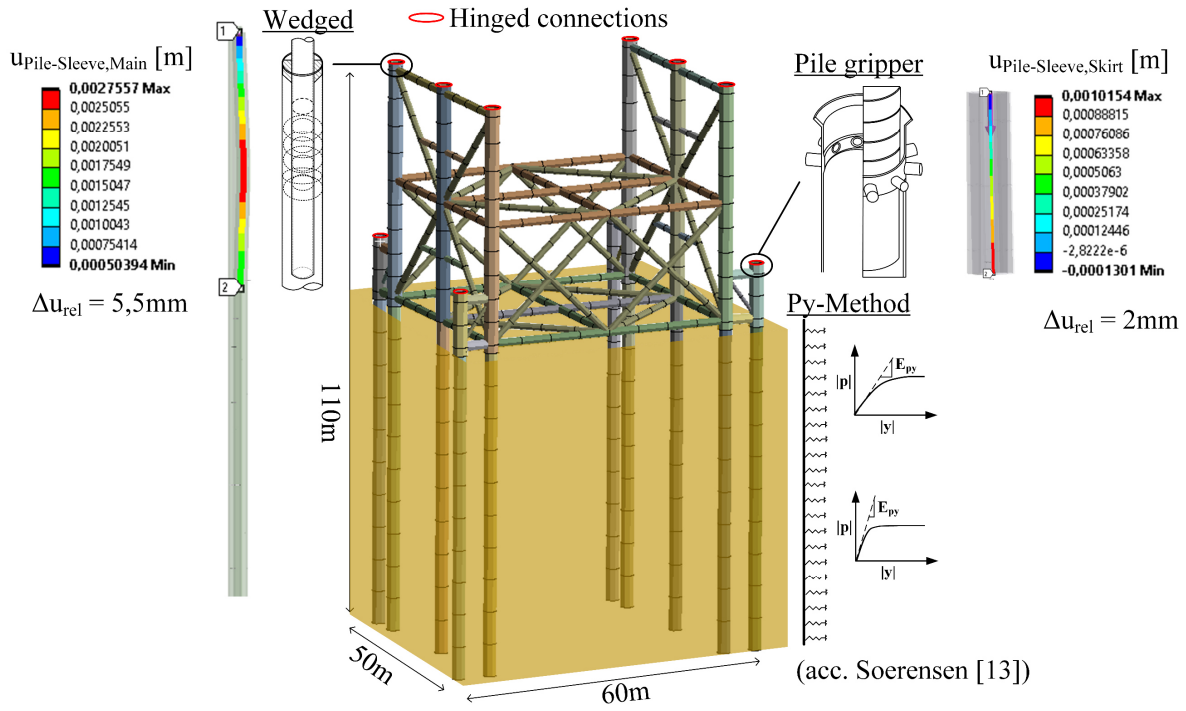

Figure 13. EAM according to elastic deformation of jacket support structure at the main piles (left) and skirt piles (right).

6. Conclusion

Independent of the type of the bottom-fixed offshore structure, EAM larger than 1mm occurred in most cases applying sea state conditions representing the common weather window for vessel operation for installation. Investigated movements are horizontal movements which can occur purely lateral or in oval shape. The efficiency of increasing structure stiffness by increasing thickness to diameter ratios or additional boundary conditions by further mechanical devices like pile gripper, are shown. To reduce EAM, increasing the thickness is more efficient than increasing the diameter, as this increases stiffness as well as wave loading. Additional mechanical fixation devices are most efficient for structures of lower stiffness. The actual trend designing offshore structures less material intense, due to increasing knowledge and experience as well as increasing structure sizes due to increasing turbines, should be taken with caution regarding EAM.

Acknowledgement

The presented results were achieved within the research project 'GREAM: Grouted joints - Influence of early age movement' funded by the German Federal Ministry for Economic Affairs and Energy (BMWi, funding sign: 0324257). The research partners were Institute for Steel Construction and Institute of Building Material Science, both at Leibniz Universität Hannover, Germany. The authors thank the BMWi for funding and all accompanying industry project partners (DNV GL, Siemens Gamesa, Wilke & Schiele Consulting GmbH, BAM and Pagel Spezial-Beton GmbH & Co. KG) for their support.

References

[1] Schaumann P, Raba A and Bechtel A 2017 *Fatigue behaviour of grouted connections at different ambient conditions and loading scenarios* Energy Procedia **137** pp. 196-203
[2] UK Department of Energy 1986 The Strength of Grouted Pile-Sleeve Connections, *Report OTH 86 210*, (London: HMSO)
[3] DNV Report No. 94-3243 – Fatigue testing of grouted connections 1994 (Oslo: DNV)

[4] DNVGL-ST-0126: Support structures for wind turbines 2016 (Oslo: DNV GL)
[5] DNVGL-ST-0126: Support structures for wind turbines 2018 (Oslo: DNV GL)
[6] Schaumann P, Lochte-Holtgreven S, Lohaus L and Lindschulte N 2010 *Durchrutschende Grout-Verbindungen in OWEA – Tragverhalten, Instandsetzung und Optimierung* (Berlin: Ernst & Sohn) Stahlbau Vol. **79**, Issue 9 pp 637-647
[7] EN ISO 19902 Petroleum and natural gas industries – Fixed steel offshore structures January 2007.
[8] Lohaus L, Schaumann P, Cotardo D, Kelma S and Werner M 2015 *Experimental and Numerical Investigations of Grouted Joints in Monopiles Subjected to Early-Age Cycling to Evaluate the Influence of Different Wave Loadings* (*Int. Offshore and Polar Engineering Conf. 2015*) Hawaii June 21-26
[9] Sumer B M and Fredsoe J 2006 *Hydrodynamics Around Cylindrical Structures* (*Advanced Series on Ocean Engineering* Vol. **26)** (London: World Scientific)
[10] Morison JR, Johnson JW and Schaaf SA 1950 *The Force Exerted by Surface Waves on Piles* (*J Pet Technol* **2)** pp.149-154
[11] Hasselmann, K. et al. 1973 *Measurements of Wind-Wave Growth and Swell Decay during the Joint North Sea Wave Project (JONSWAP)* (*Deutsche Hydrographische Zeitschrift Suppl.* A8) **12** pp. 1-95
[12] Young-Bo S 2007 *Geometrical effect on the stress distribution along weld toe for tubular T- and K-joints under axial loading* (*Journal of Constructional Steel Research* Vol. 63) Issue 10 pp. 1351-1360
[13] Sørensen S P H 2012 *Soil-structure interaction for non-slender large-diameter offshore monopiles*. (Aalborg: River Publishers) PhD thesis Aalborg University Denmark Dept. of Civil Engineering
[14] Thieken K, Achmus M and Lemke K 2015 *A new static p-y approach for piles with arbitrary dimensions in sand* (*Geotechnik* Vol. **38)** (Berlin: Ernst & Sohn) Issue 4 pp.267-288